

Fabrication of a Resonant Photoacoustic Cell for Samples Study

J.C. Kapil, S.K. Joshi, and A.K. Rai

G.B. Pant University of Agriculture & Technology, Pantnagar-263 145

ABSTRACT

Nondestructive treatment of a sample in photoacoustic spectroscopy is helpful in the study of thermal and optical properties of ice and snow. In the present study, a low-temperature resonant photoacoustic cell, based on Helmholtz resonator model, has been designed and fabricated for the study of samples like ice or snow. Its performance has also been studied using carbon black as a standard sample and various other samples like water, ice, glass, plexi-glass, polycarbonate, etc. Thermal diffusivity of ice, water, and many other transparent materials has been determined by varying chopping frequency and recording corresponding phase changes in the photoacoustic signal. The results obtained are in good agreement with those predicted by Rosencwaig-Gersho (R-G)¹ theory.

Keywords: Photoacoustic spectroscopy, thermal diffusivity, low-temperature photoacoustic cell, resonant photoacoustic cell, Helmholtz resonator, ice, plexi-glass, photoacoustic signal, acoustic cell, nondestructive testing

1. INTRODUCTION

Photoacoustic spectroscopy has emerged as a nondestructive technique for studying any sample in the form of solids, liquids, semi-solids, gels, etc.^{1,2} It offers special advantages over other conventional spectroscopic methods since it can be applied even when the samples are transparent, opaque or highly scattering. Thus, physical properties of ice and snow can be studied using this spectroscopic tool. Ice and snow are not only the most familiar and important solid materials for human being but are also associated with avalanche activities in Himalayan region, which is important from the defence point of view. Ice and snow are typical examples of hydrogen-bonded crystals³ which exist below 0 °C and a little change in the ambient condition, ie,

temperature, pressure, external disturbances, etc., changes its structure. Snow is a composite phase of ice crystals, water vapours, and air and is found in over six thousands crystal types. Study of physical properties of ice and snow by conventional spectroscopic methods is a very difficult and challenging task. The nondestructive treatment of samples in photoacoustic spectroscopy is helpful in the pursuit of such a study.

Photoacoustic spectroscopy is based on the principle that when a chopped monochromatic light falls on a sample enclosed in a photoacoustic cell, heat waves are generated as a result of quantum mechanical process, known as nonradiative de-excitation process². The heat thus generated in this process results in the pressure change in the coupling gas, which

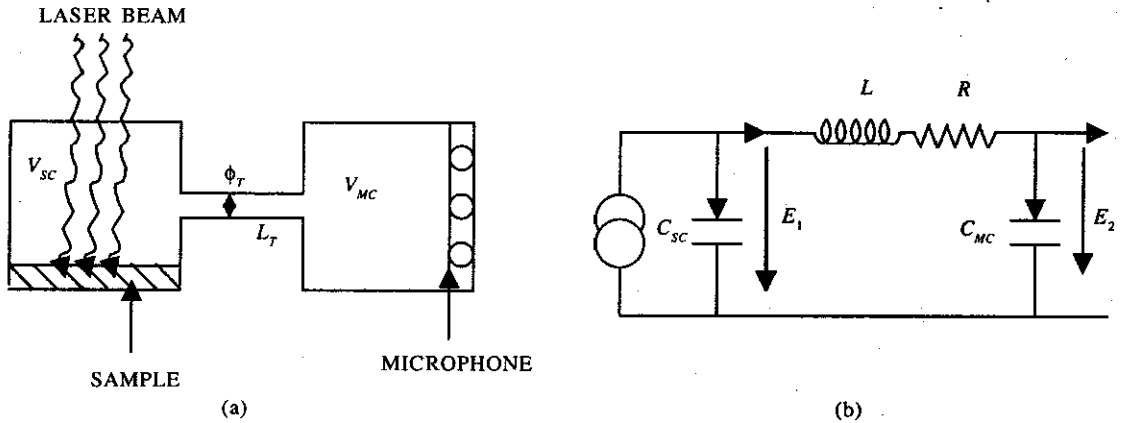


Figure 1. Helmholtz resonator model: (a) photoacoustic cell and (b) electrical equivalent circuit

gives rise to an acoustic signal. This signal is detected by a pressure transducer (electret microphone), subsequently amplified and finally recorded as a photoacoustic signal. The amplitudes of photoacoustic signals for constant light absorption depend on the physical size of the photoacoustic cell through the diffusion process. The thermal diffusion length of the coupling gas is very important for signal detection. For a spatial separation x between the sample surface and the detector, the photoacoustic signal has substantial value within the distance $0 \leq x \leq \pi\mu_g$ and is damped out beyond the distance $\pi\mu_g$.

For the study of ice and snow, low-temperature photoacoustic cells are required as these materials exist below 0°C . There are two different designs of low-temperature photoacoustic cells⁴:

- (a) Nonresonant photoacoustic cell, in which the whole cell, including microphone chamber, is cooled down to the required temperature.
- (b) Resonant photoacoustic cell, in which the sample chamber is cooled down and the microphone chamber is placed at room temperature.

But in the case of nonresonant photoacoustic cell, sensitivity and frequency response of the electret's microphone decreases with decreasing temperature⁵, and is also affected by the vapour deposition on the electret's diaphragm.

Hence for the study of samples like ice or snow, the use of a resonant photoacoustic cell is

much better than and preferable to a nonresonant photoacoustic cell. In the present work, a low-temperature resonant photoacoustic cell has been fabricated to study the physical properties of the samples like ice or snow.

2. THEORETICAL BACKGROUND

Theory of a resonant photoacoustic cell may be explained by an extended Helmholtz resonator (EHR) model^{4,6}. An extended Helmholtz resonator in its simplest form comprises two chambers having volumes V_{SC} and V_{MC} and connected to a small cylindrical tube, used as acoustic transmission line of the length L_T and of diameter ϕ_T , has been shown in Fig. 1(a). Gas column in the tube performs forced oscillations imposed by an external pressure modulation. Gas in the tube is considered to move like a rigid piston without any compression. For a displacement X of the gas piston, the equation of motion is given by⁶

$$P(t) = \frac{\rho L_T}{A} \ddot{X} + R_{ac} \dot{X} + \rho C_0^2 \left(\frac{1}{V_{SC}} + \frac{1}{V_{MC}} \right) X \quad (1)$$

where $P(t)$ is the change in gas pressure, ρ is the density of the coupling gas, C_0 is the acoustic velocity, A is the area of cross section of the connecting tube, and R_{ac} is the acoustic resistance.

The electrical analogue of the Helmholtz resonator may be represented by an equivalent LCR circuit as shown in Fig.1(b) and the

equivalent electrical analogue of the Eqn (1) can be written as

$$E(t) = L\ddot{Q} + R\dot{Q} + \frac{1}{C}Q \quad (2)$$

where Q is the electric charge, $E(t)$ is the periodic electromotive force, and R, L, C are the electrical resistance, inductance, and capacitance, respectively.

It is obvious that an electro-acoustic analogy can be established in the resonant photoacoustic cell and an LCR circuit. Hence, from Eqns (1) and (2), one can define acoustic inductance and acoustic capacitance as

$$L = \rho \frac{L_T}{A} \quad \text{and} \quad \frac{1}{C} = \rho C_0^2 \left(\frac{1}{V_{SC}} + \frac{1}{V_{MC}} \right)$$

Thus, the resonance frequency of the Helmholtz resonator can be determined from the resonance frequency of an LCR circuit, ie,

$$\omega_R = \frac{1}{\sqrt{LC}}$$

Now, substituting the equivalent values of L and C by their acoustic analogues, one gets:

$$\omega_R = \sqrt{\frac{AC_0^2}{L_T(1/V_{SC} + 1/V_{MC})}} \quad (3)$$

where

$$A = \frac{\pi \phi_T^2}{4}$$

Thus, one gets the resonance frequency of the resonant photoacoustic cell as

$$f_R = \frac{C_0}{4\sqrt{\pi}} \phi_T \sqrt{\frac{(V_{MC} + V_{SC})}{(V_{MC} V_{SC} L_T)}} \quad (4)$$

Applying the end corrections⁷, one gets the resonance frequency f_R as

$$f_R = \frac{C_0}{4\sqrt{\pi}} \phi_T \sqrt{\frac{(V_{MC} + V_{SC})}{\{V_{MC} V_{SC} (L_T + 0.85 \phi_T)\}}} \quad (5)$$

3. EXPERIMENTAL PROCEDURE

A resonant photoacoustic cell has been designed and fabricated at the G.B. Pant University of Agriculture and Technology, Pantnagar, for the study of samples like ice or snow, in a variable temperature range of -40°C to room temperature (Fig. 2). The main body of the photoacoustic cell is made of purified aluminum after casting into the desired dimensions. The outer dimensions of the photoacoustic cell are $10.0 \text{ cm} \times 7.0 \text{ cm} \times 7.5 \text{ cm}$ as shown in Fig. 2. Typical values of cell parameters used in the fabrication of the photoacoustic cell are:

$$V_{SC} \approx 0.92 \text{ cm}^3, \quad V_{MC} \approx 0.87 \text{ cm}^3, \quad V_T \approx 0.69 \text{ cm}^3, \\ L_T \approx 7.5 \text{ cm}, \quad \text{and} \quad \phi_T \approx 0.2 \text{ cm}$$

where the symbols have their usual meanings as described in the Section 2 and values are the best fitted for an optimised photoacoustic cell⁷. The calculated resonant frequency of the cell designed is 542 Hz. For optimising the photoacoustic cell efficiency³, the following points have been considered:

- (a) Diameter of the tube has been chosen such that no thermo-viscous damping prevails, ie, $\phi_T \geq 1 \text{ mm}$.
- (b) Length L_T of the tube has been kept as small as possible.
- (c) Distance between the sample and the window is approximately equal to the thermal active layer ($2\pi \mu_g$) in the coupling gas.

In the fabrication of the photoacoustic cell, a double windowed (quartz) hollow box has been used for providing optical access and thermal insulation to the sample chamber⁸⁻¹⁰. Electret microphone is mounted in a plexy-glass chamber (Fig. 2), which provides insulation to the microphone from the surrounding noise and the sample chamber is sealed by a parafilm 'M' o-ring. The acoustic signal generated

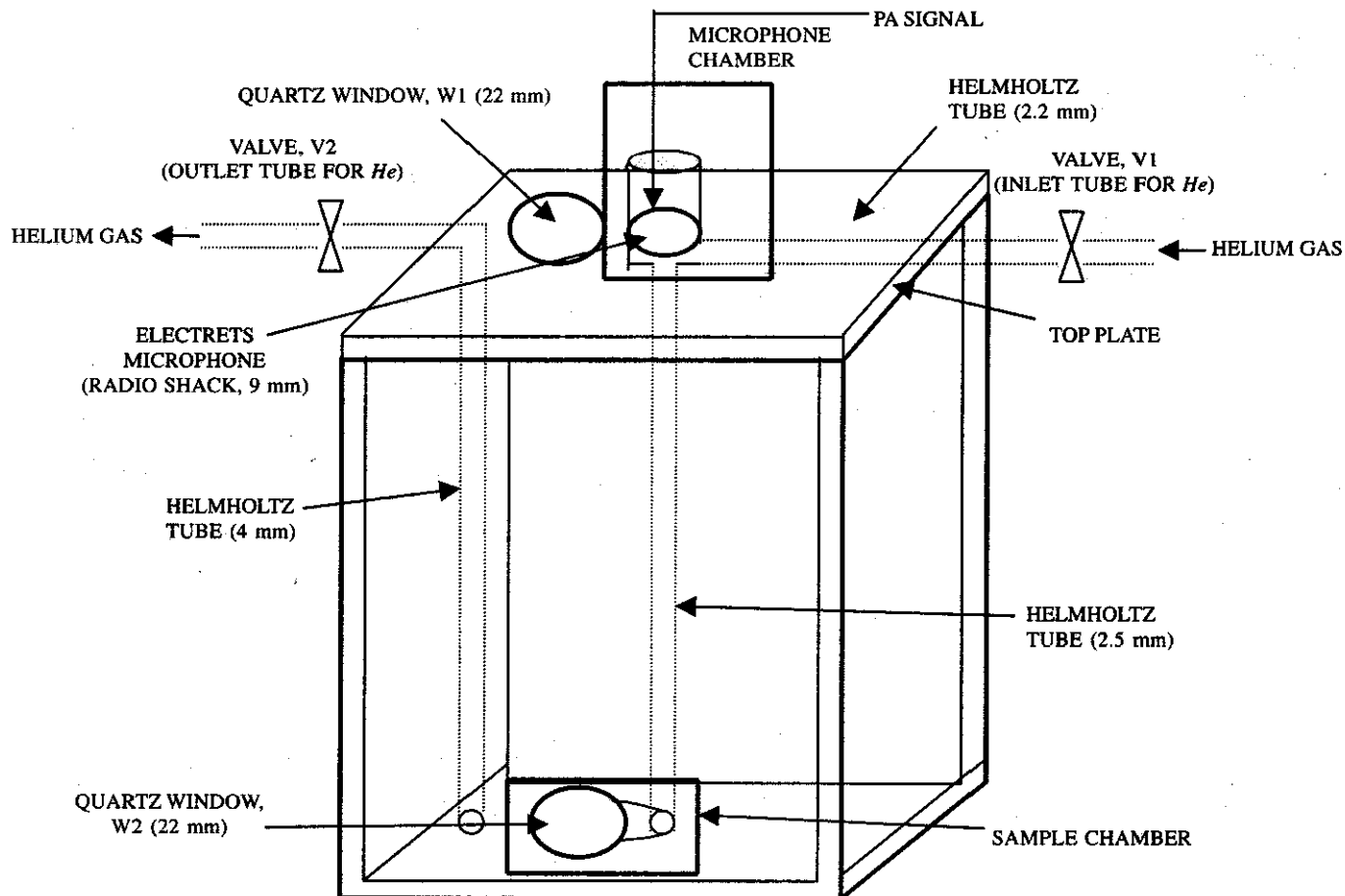


Figure 2. Low-temperature resonant photoacoustic cell

by optical absorption is transmitted to the electret microphone kept at room temperature, via a stainless steel tube of 2 mm diameter. The entire base and the side faces of the photoacoustic cell to be in contact of a low-temperature cavity which has been specially made for the study of ice or snow. Eutectic method of cooling the system is preferred to liquid nitrogen cooling, because noise is produced in liquid nitrogen due to the bubbling. In the eutectic method, the eutectic refrigerant is filled in the container surrounding the desired cavity and the cooling coils are merged in it. The whole system is thermally insulated from the surrounding. Thermocouples are used for the measurement of the temperature. For the study of ice or snow, a variable temperature (between $-30\text{ }^{\circ}\text{C}$ to room temperature) can be obtained.

Schematic diagram of the experimental setup used in the present study is shown in Fig. 3. Light beam from a 25 mW polarised radiation (632.8 nm) of a *He-Ne* laser (510 P, Aerotech USA) has been used as the excitation source. The laser light is modulated by a mechanical chopper (Stanford SR 540) and is directed to the sample compartment of the photoacoustic cell. Photoacoustic signal from the microphone (radio shack) mounted on the microphone chamber is then amplified and fed to lock-in-amplifier (Stanford SR 530) whose reference channel is connected with a chopper for phase-sensitive detection. This permits the measurement of the photoacoustic signal amplitude and the phase angle wrt the reference signal from the frequency chopper.

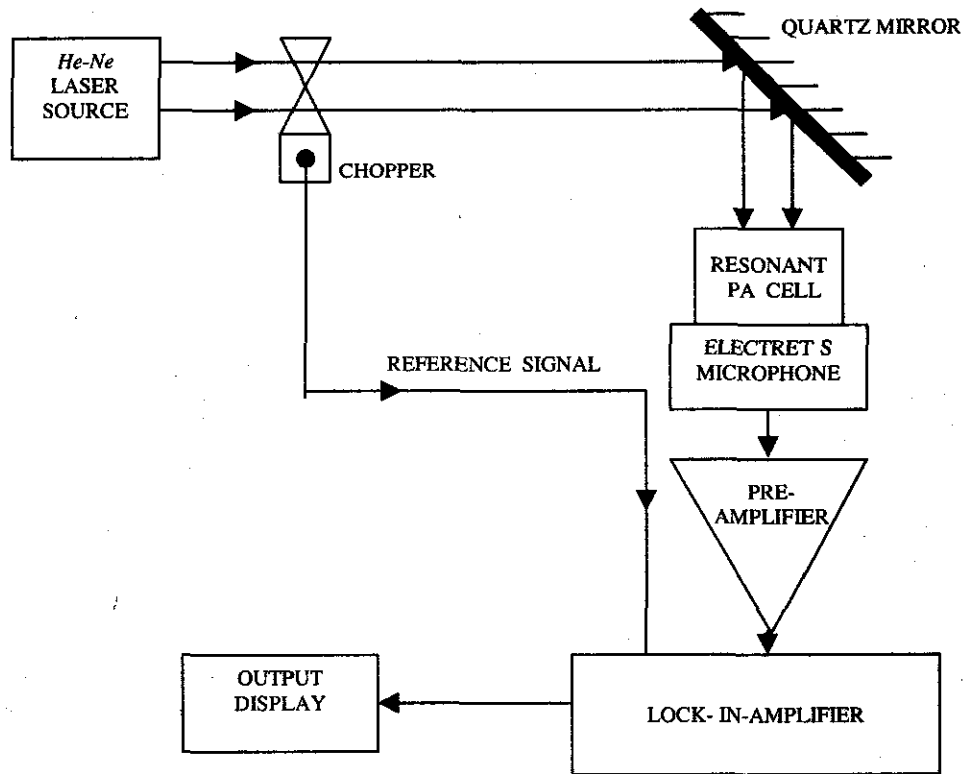


Figure 3. Schematic diagram of photoacoustic spectrometer

The present study has been carried out to determine the thermal diffusivity of distilled water, ice, glass, plexi-glass, polycarbonate by measuring the phase lag when the periodic heat wave (which is generated at the bottom of the sample) diffuses across the sample surface and the incident modulated radiation.

Experiments have been performed at various modulation frequencies by changing the chopper frequency from 5 Hz to 400 Hz. Base of the sample cup is coated with a very thin layer of matt-black enamel [above which the optically transparent samples like water, ice, glass, plexy-glass were kept for recording the photoacoustic spectra (Fig. 4)], which has high absorptivity and is considered to have a negligible effect on the thermal characteristics of the samples used^{11,12}.

4. RESULTS & DISCUSSION

Frequency dependence of amplitude and phase of the photoacoustic signal have been obtained by front surface illumination^{13,14} of samples using a

25 mW *He-Ne* laser at wavelength 632.8 nm as shown in the Fig. 4. To check the performance of the present photoacoustic cell, parametric studies have been performed using carbon black as a standard sample. The phase shift and the amplitude of the photoacoustic signal have been recorded by varying chopping frequency from 5 Hz to 400 Hz. Variation of the photoacoustic signal strength [Fig. 5(a)] and the phase shift [(Fig. 5(b))] with chopping frequency of carbon black are in good agreement with the Rosencwaig-Gersho (R-G) theory^{1,2,15}. As a result of absorption of the chopped laser beam by the sample, periodic heat waves are generated within the sample which give rise to the photoacoustic signal in the adjacent coupling gas. A phase lag occurs during the diffusion of heat waves within the sample in the photoacoustic signal wrt the reference signal, which depends on the thermal properties of the sample. For optically transparent samples, having very low absorption coefficient, like water, ice, glass, etc, a black enamel-coated tin sheet has been used as strongly absorbing and

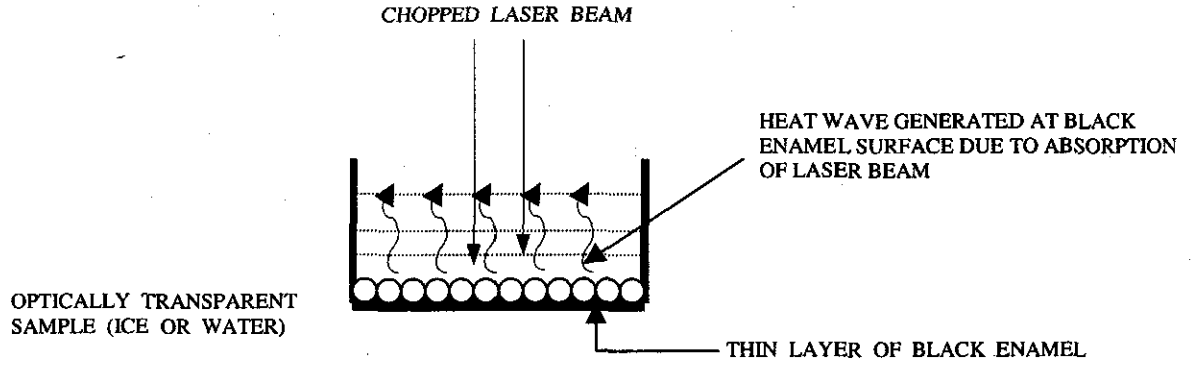


Figure 4. Diffusion of heat in an optically transparent sample after absorption of chopped laser by black enamel coating of the sample cup.

backing material as shown in the Fig. 4. Heat waves generated by the absorption of laser beam by the black enamel propagate in the sample medium (Fig. 4). During this process, a phase shift between the heat waves at the sample surface and the reference incident laser beam, is produced. The phase shift in the photoacoustic signal depends on the thermal properties of the sample, which is useful in the determination of thermal diffusivity of the sample used¹³. Acoustic waves are generated at the sample gas interface^{1,3} within a very small distance $x \leq \pi\mu_g$,

where μ_g is the thermal diffusion length of the coupling gas. Since the phase measurement depends on the photoacoustic cell design and measurement system, a phase calibration has been performed by measuring the phases as a function of chopping frequency using a thermally thick carbon black sample¹¹ of the thickness 3.0 mm. Phases were also recorded for an empty sample cup by varying the chopping frequency. The phase lag $\Delta\theta$ is then found by subtracting the phase of empty cup from the phase of sample-filled cup, hence, the phase

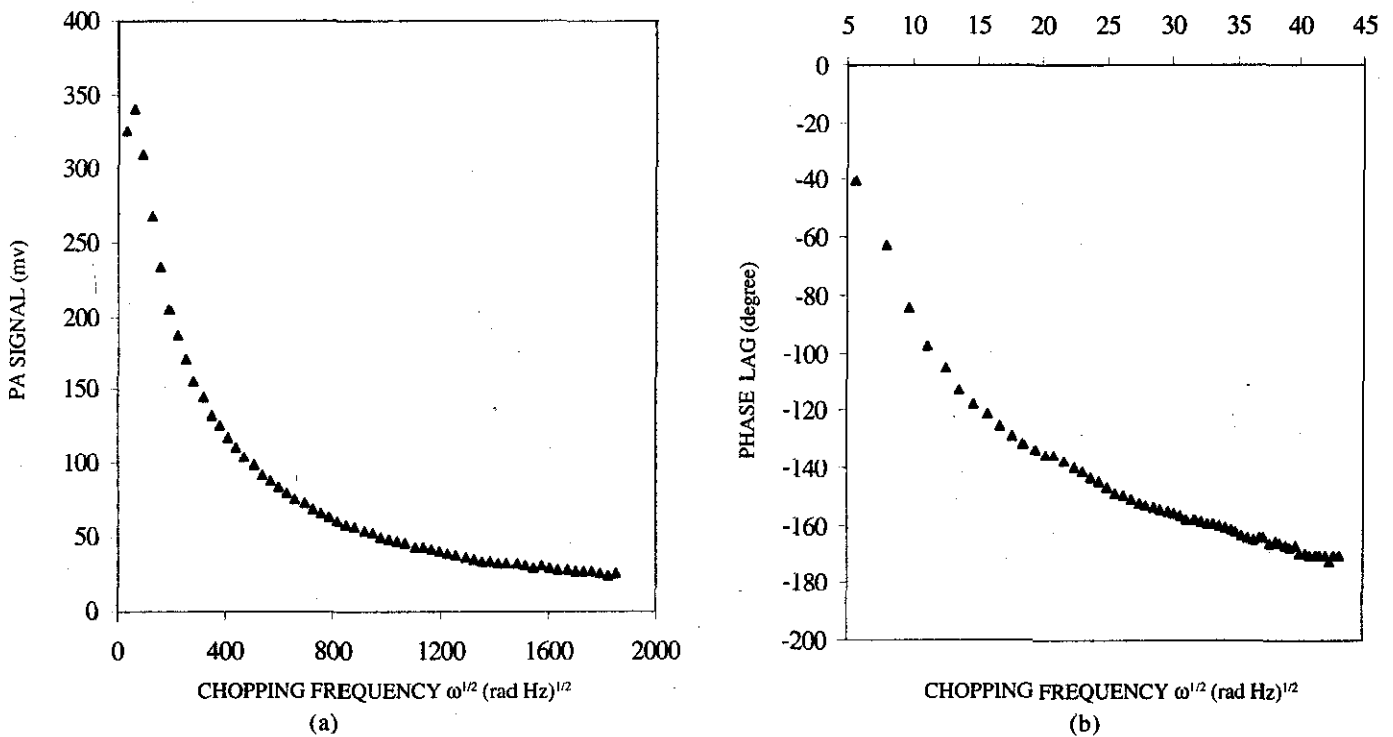


Figure 5. Variation of (a) amplitude and (b) phase lag ($\Delta\theta$) of carbon black with chopping frequency

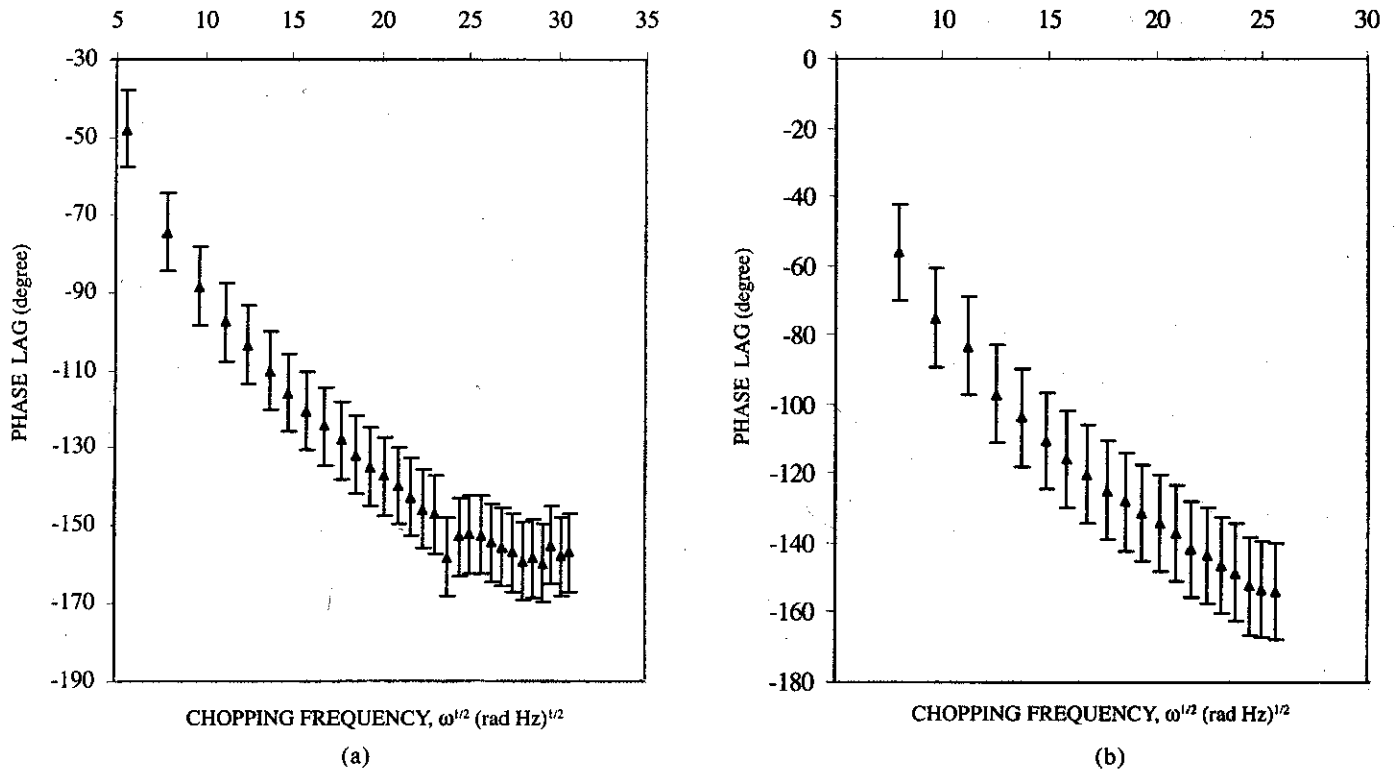


Figure 6. Variation of phase lag with chopping frequency (ω)^{1/2} of: (a) distilled water and (b) ice

difference $\Delta\theta$ is recorded as a function of chopping frequency ranging from 5 Hz to 150 Hz.

After testing the performance of photoacoustic cell, this experimental setup has been used to determine the thermal diffusivity of water and ice from the following relation^{11,12}:

$$\Delta\theta = x(\omega/2\alpha)^{1/2} \quad (6)$$

where x is the sample thickness, ω is the chopping frequency, and α is the thermal diffusivity of the sample.

Figures 6(a) and (b) show variation of phase lag with chopping frequency for distilled water and ice of sample thickness 0.2 mm. A plot between $\Delta\theta$ and $\sqrt{\omega}$ is a linear relation, which follows the R-G theory¹. At low modulation frequencies, phase difference is a positive quantity, while at higher modulation frequencies, it is going negative, which is in good agreement with the R-G theory¹ and with results obtained by Lachaine¹⁵. Generation of the photoacoustic signal by the absorption of the

radiation depends on the thermal diffusion length of the periodic heat wave. Dependence¹ of the thermal diffusion length (μ) with the chopping frequency (ω) is:

$$\mu = (2\alpha / \omega)^{1/2} \quad (7)$$

At low chopping frequencies, thermal diffusion length is large, hence, both the sample and the backing material contribute to the generation of the photoacoustic signal, while at higher modulation frequencies, thermal diffusion length is small, hence, only the sample contributes in the generation of the photoacoustic signal. At the interface of the sample and the backing material, there is a bend (nonlinearity) in the $\Delta\theta - \sqrt{\omega}$ plot, and thereafter, it shows sample properties only. Thermal diffusivities of water and ice have been calculated using Eqn (6) and the slope of Figs 6(a) and (b). The results obtained are compared with the previously reported values¹⁶ in the Table 1. For checking the validity of this technique, other optically transparent samples¹⁷⁻¹⁸ like glass, plexi-glass, and polycarbonate have also

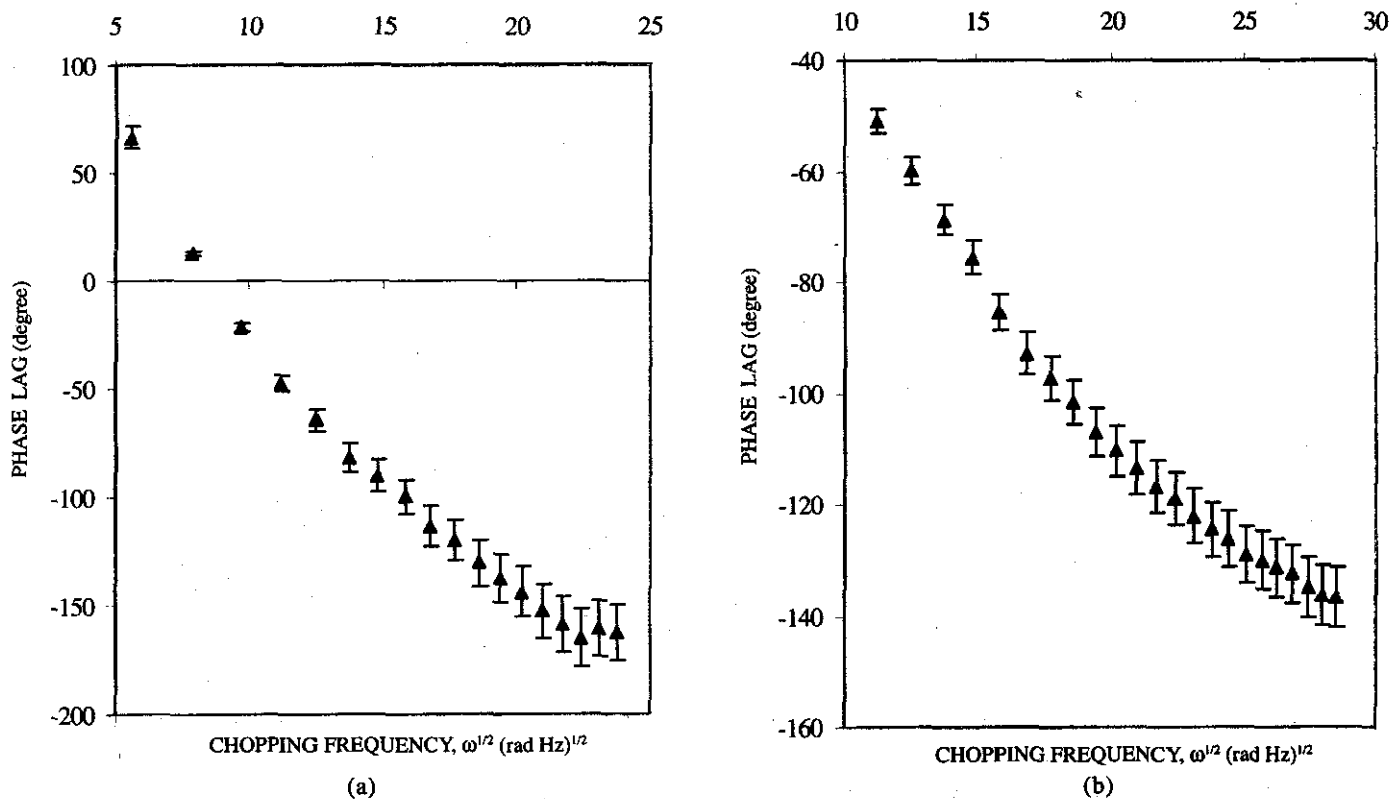


Figure 7. Variation of phase lag with chopping frequency: (a) plexi-glass and (b) glass

been studied, and the results thus obtained are shown in the Table 1.

5. CONCLUSION

The study carried out for the design and fabrication of a low-temperature photoacoustic cell and the results obtained will be helpful in the study of many thermal and optical properties of the complex materials like snow, ice, etc which is quite useful in the avalanche forecasting. Because of the nonavailability of the snow at Pantnagar, spectro-

scopic study of the snow could not be carried out at the G.B. Pant University of Agriculture & Technology, hence, further work will be carried out at the Snow & Avalanche Study Establishment (SASE), Chandigarh.

ACKNOWLEDGEMENT

This research is a sequel to the findings based on the project, entitled, 'Study of physical properties of snow with photoacoustic spectroscopy', collaborated by the SASE, Chandigarh, and funded by ER & IPR (DRDO), New Delhi. The authors are thankful to the Director SASE for taking keen interest in this project and providing all the facilities.

Table 1. Thermal diffusivities of different samples obtained by photoacoustic technique

Sample type	Thermal diffusivity	
	Photoacoustic method	Reported ¹⁶ in the literature
Glass plate	0.00440	0.00620
Distilled water	0.00130	0.00165
Ice	0.01230	0.01350
Plexi-glass	0.00096	0.001276
Polycarbonate	0.00640	Not available

REFERENCES

1. Rosencwaig, A. & Gersho, A. Theory of photoacoustic effect with solids. *J. Appl. Phys.*, 1976, 47(1), 64-69.
2. Tam, A.C. Pulsed optoacoustic spectroscopy of condensed matter. *Rev. Mod. Phys.*, 1986, 58, 381.

3. Seki, Masami; Kobayashi, Koichi & Nakahara, Jun'ichiro. Optical spectra of hexagonal ice. *J. Phys. Soc. Jpn.*, 1981, **50**(8), 2643-648.
4. Klein, K.; Pelzl, J. & Fütterer, H. Proceedings of the 1st International Conference on the Photoacoustic Effect, Germany, 23-26 February 1981. pp. 412-19.
5. Rai, V.N. Photoacoustic spectroscopy of some materials. PhD Thesis, 1983. pp.-53-55.
6. Bechthold, P.S. *In* Proceedings of the 1st International Conference on the Photoacoustic Effect, Germany, 23-26 February 1981. pp. 375-11.
7. Coufal, H.; Möller, U. & Schneider, S. *In* Proceedings of the 1st International Conference on the Photoacoustic Effect, Germany, 23-26 February 1981. pp. 420-30.
8. Aamodt, L.C.; Murphy, J.C. & Parker, J.G. Size considerations in the design of cells for photoacoustic spectroscopy. *J. Appl. Phys.*, 1977, **48**(3) 927-33.
9. Murphy, J.C. & Aamodt, L.C. Photoacoustic spectroscopy of luminescent solids: Ruby. *J. Appl. Phys.*, 1977, **48**(8), 3502-509.
10. Aamodt, L.C. & Murphy, J.C. Size consideration in design of cells for photoacoustic spectroscopy. II. Pulsed excitation responses. *J. Appl. Phys.*, 1978, **49**(6), 3036-045.
11. Adams, M.J. & Kirkbright, G.F. Optoacoustic effect and thermal diffusivity. *Analyst*, 1977, **102**, 281-92.
12. Adams, M.J. & Kirkbright, G.F. Thermal diffusivity and thickness measurements for solid samples utilising optoacoustic effect. *Analyst*, 1977, **102**, 678-82.
13. Leporture, F.; Fournier, D. & Boccara, A.C. *In* Photoacoustic and photothermal phenomena, III, edited by D. Bicanic. Springer, Berlin, 1992. pp. 717.
14. Singh, J. & Ram, R.S. Thermal diffusivity of nickel mangnite compound using a photoacoustic method. *Phys. Status. Solidi.*, 1996, **158**, 73-78.
15. Lachaine, Andre. Thermal analysis by photoacoustic phase measurements: Effect of sample thickness. *J. Appl. Phys.*, 1985, **57**(11), 5075-077.
16. Touloukian, L.R.; Powell, R.W., Ho, C.Y., & Nicolaus, M.C. *In* Thermal diffusivity. Plenum, New York, 1973. pp. 390.
17. Patel, C.K.N. *In* Proceedings of the 1st International Conference on the Photoacoustic Effect, Germany, 23-26 February 1981. pp. 21-39.
18. Pessoa, O.(Jr); Cesar, C.L.; Patel, N.A.; Vergas, H.; Ghizoni, G.C. & Miranda, L.C.M. Two beam photoacoustic phase measurements of the thermal diffusivity of solids. *J. Appl. Phys.*, 1986, **59**(4), 1316-318.